very rapidly at low flow rates. Values corresponding to the three stages of the batch reaction appear over a very narrow flow rate range as is shown in Figure 7. The simulations are very sensitive in this region, and it may be that the observed noisy oscillations in our and Simoyi's[15] CSTR experiments result from an extreme sensitivity of the experimental system to environmental perturbation. The effect of mixing[31] experimentally and in this model should be carefully investigated. The CSTR experiments also need to be repeated with more precisely controlled pumps.

Acknowledgment. This work was supported by the National Science Foundation under Grant CHE 8822886. We thank László Györgyi for helpful discussions and the University of Montana Computer and Information Services for computing facilities.

Registry No. BrO_3^-, 15541-45-4; SCN^-, 302-04-5; Fe^{3+}, 20074-52-6; CN^-, 57-12-5.

(31) Györgyi, L.; Field, R. J. *J. Chem. Phys.* **1989**, *91*, 6131.
(32) Fogelman, K. D.; Walker, D. M.; Margerum, D. W. *Inorg. Chem.* **1989**, *28*, 986.
(33) Yiin, B. S.; Margerum, D. W. *Inorg. Chem.* **1990**, *29*, 1559.

Confirmation of High Flow Rate Chaos in the Belousov–Zhabotinsky Reaction

Laszlo Györgyi,[†,‡] Richard J. Field,[*,†] Zoltan Noszticzius,[§,∥] William D. McCormick,[§] and Harry L. Swinney[*,§]

Department of Chemistry, University of Montana, Missoula, Montana 59812, Center for Nonlinear Dynamics and Department of Physics, University of Texas at Austin, Austin, Texas 78712, Institute for Inorganic and Analytical Chemistry, Lorand Eotvos University, Budapest H-1528, Hungary, and Department of Chemical Physics, Technical University of Budapest, Budapest H-1521, Hungary *(Received: July 23, 1991)*

Past experiments and simulations on the Belousov–Zhabotinsky (BZ) reaction clearly demonstrated the existence of chaos in stirred flow reactors at low flow rates. However, the existence of chaos at high flow rates has remained the subject of controversy. The controversy is resolved by the present experiments at high flow rates, which accurately reproduce the complex sequence of periodic, complex periodic, and chaotic states observed by Hudson and co-workers (Hudson et al., 1979; Hudson and Mankin, 1981); the flow rates observed here for the different dynamical regimes agree with those of Hudson et al. within a few percent. This striking reproducibility of the complex periodic and chaotic dynamics is found to be insensitive to stirring rate, size of the reactor, purity of the reagents, temperature, and type of pumping (peristaltic or piston pumps, premixed or nonpremixed feeds). Moreover, the observed sequence is reproduced qualitatively by a four-variable model of the BZ reaction. Thus, this work provides definitive evidence for the existence of deterministic chaos in the BZ reaction at high flow rates. We conclude that past descriptions of aperiodic behavior at high flow rates in terms of various stochastic mechanisms, including incomplete mixing or switching between adjacent periodic states, are inappropriate for the conditions of the Hudson's experiments.

I. Introduction

The most striking examples of the occurrence of nonlinear dynamical phenomena[1] in chemical systems maintained far from equilibrium have been provided by the oscillatory Belousov–Zhabotinsky[2] (BZ) reaction. Periodic, quasiperiodic, and aperiodic oscillations, intermittency, phase-locking, bistability, hysteresis, excitability, and spatial pattern formation have all been observed under appropriate conditions. We are concerned here with the question of the existence of deterministic chaos when the BZ reaction is run in a continuous-flow, stirred tank reactor (CSTR).

The CSTR is a convenient and versatile tool[3] for studying the dynamical behavior of chemical systems. The major reactants are pumped into a vigorously stirred reactor at a particular flow rate while the reaction mixture flows out at the same rate. The system is thus maintained away from equilibrium, and the dynamics of the flow may couple with the chemical dynamics. A further advantage of CSTR experiments is that true stationary states can be obtained and their characteristics, as well as the bifurcations separating them, can be explored in detail. The dynamical behavior of the system can thus be determined by searching the space of the main control parameters: flow rate, temperature, and reagent concentrations in the feed streams. The flow rate is usually used as the bifurcation parameter at a particular temperature and set of feed stream concentrations because it is easy to control.

Under typical experimental circumstances the BZ reaction shows an oxidized steady state at high flow rates, a reduced steady state at low flow rates, and, often, periodic oscillations at intermediate flow rates. Residence times range from minutes to hours. Aperiodic oscillations are also possible and were first found at high CSTR flow rates by Schmitz et al.[4] and further studied by Hudson and co-workers.[5,6] Many more aperiodic regions have been discovered since then near the bifurcations between steady state and oscillatory behavior at both high and low flow rates. The aperiodicity was shown to be deterministic chaos by examination of the attractor in the reconstructed phase space of the system, by return maps taken from Poincaré sections of that

* Authors to whom correspondence should be addressed.
† University of Montana.
‡ Lorand Eotvos University.
§ University of Texas.
∥ Technical University of Budapest.

(1) (a) *Oscillations and Traveling Waves in Chemical Systems*; Field, R. J., Burger, M., Eds.; Wiley-Interscience: New York, 1985. (b) Gray, P.; Scott, S. K. *Chemical Oscillations and Instabilities. Non-linear Chemical Kinetics*; Clarendon Press: Oxford, U.K., 1990. (c) *Waves and Patterns in Biological and Chemical Media*; Swinney, H. L., Krinsky, V. I., Eds.; North-Holland: 1991; Physica D 49.
(2) (a) Belousov, B. P. In *Sbornik Referatov po Radiatsionnoi Meditsine*; Medgiz: Moscow, 1958; p 145 (in Russian). (b) Zhabotinsky, A. M. *Biofizika* **1964**, *9*, 306 (in Russian).
(3) De Kepper, P.; Boissonade, J. In *Oscillations and Traveling Waves in Chemical Systems*; Field, R. J., Burger, M., Eds.; Wiley-Interscience: New York, 1985; p 223.
(4) Schmitz, R. A.; Graziani, K. R.; Hudson, J. L. *J. Chem. Phys.* **1977**, *67*, 3040.
(5) Hudson, J. L.; Hart, M.; Marinko, D. *J. Chem. Phys.* **1979**, *71*, 1601.
(6) Hudson, J. L.; Mankin, J. C. *J. Chem. Phys.* **1981**, *74*, 6171.

0022-3654/92/2096-1228$03.00/0

attractor, and by calculation of the largest Lyapunov exponent and dimension of the attractor.[6,7]

There has been some controversy concerning the mechanistic source of chaos in the BZ reaction.[8] Two reasons for this uncertainty were the lack of independent reproduction of the various experiments and the inability of chemically reasonable models of the BZ reaction to reproduce the experimentally observed aperiodicity. Stochastic[9] and mixing[10] effects have been invoked in an attempt to solve these problems and still must be considered for cases in which the attractors and their return maps do not exhibit the characteristic features of deterministic chaos. This controversy recently has been resolved, however, in the case of the low flow rate chaos by independent reproduction[9] of some features of the original experiments[7] and by their successful simulation[11] with models of the BZ reaction. The source of the high flow rate aperiodicity, however, has remained problematical. Although several experiments[4-7,12] and simulations[13] supported the existence of deterministic chaos at high CSTR flow rates, recent experiments by Münster and Schneider[9] seemed to indicate that the observed aperiodicity was caused by noise-driven transitions of the system between neighboring periodic orbits. Furthermore, no particular examples of high flow rate aperiodicity have been reproduced in another laboratory. This uncertainty is further aggravated by the findings of Noszticzius et al.[14,15] that trace contaminants in the major reagents can cause significant changes in the sequence of bifurcations observed at low CSTR flow rates.

Here we reproduce in remarkable detail one of the first high flow rate experiments and study its sensitivity to trace impurities, to variations in CSTR temperature, volume, and stirring rate, and to the CSTR feeding mode, i.e., peristaltic vs piston pump. We also show that the experimental results may be reproduced by simulations based on a recent model of the BZ reaction.

II. Experimental Section

A. Materials. Malonic acid (Eastern) was recrystallized from acetone. This is a modification of our previous method in which a mixture of acetone and chloroform was used.[14] The change was necessary because our recent sample contained malonic acid–iron complexes (both iron(II) and iron(III), altogether about 7 ppm w/w), which were difficult to remove with the previous technique. In addition, a trace amount of free sulfuric acid also contaminated our sample. It was important to neutralize that free sulfuric acid to avoid a formation of colored condensation products of acetone during the recrystallization procedure. Thus, 600 g of malonic acid and 1 g of NaOH were dissolved in 690 mL of acetone (Mallinckrodt a.r.) on a hot plate. The hot solution was filtered through a glass filter paper to remove some insoluble contaminants (mostly $CaSO_4$ and activated charcoal) from the malonic acid solution. The glass filter paper was placed into a prewarmed funnel and was wetted with acetone prior to filtration to avoid crystallization inside the funnel. The filtrate was cooled to laboratory temperature (~25 °C), and the malonic acid crystals were collected by a second filtration. The crystals were washed with 1050 mL of chloroform (Mallinckrodt a.r.). The washing chloroform was mixed with the acetone filtrate to precipitate a second part of the malonic acid that remained dissolved in acetone. Most of the iron contamination was still present in the acetone solution and was precipitated by chloroform together with the second part of the malonic acid. Thus, the first part of the malonic acid was relatively free of iron (yield: ~360 g with 1.5 ppm of iron w/w), while the second part contained most of it (yield: ~160 g with 22 ppm of iron w/w). The iron-contaminated malonic acid can be used in other experiments (e.g., chemical wave experiments with ferroin as a catalyst). In our present experiments we used the first part, which was relatively free of iron. The iron content can be decreased below 0.5 ppm by a second recrystallization employing the same method. Experiments with this highly purified sample, however, produced the same results as those with malonic acid recrystallized only once. Thus, in most of our experiments we used malonic acid recrystallized from acetone only once. $NaBrO_3$ (Fischer reagent grade) was recrystallized from water to remove bromide traces. $Ce_2(SO_4)_3 \cdot 8H_2O$ (Aldrich 99.999%) was used without further purification.

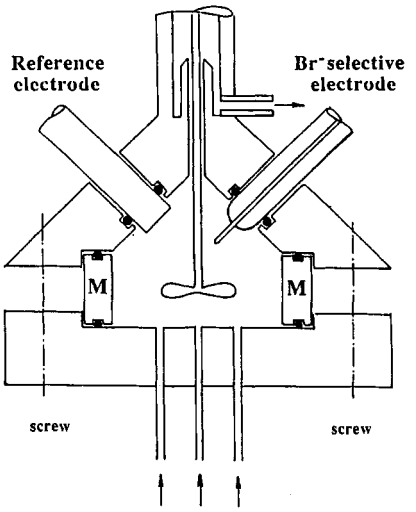

Figure 1. Schematic drawing of the cylindrical Plexiglas reactor. The reactor volume and geometry could be modified by changing the middle part marked with M in the figure. This construction is somewhat different from Hudson's reactor: he used a cylindrical reactor with two baffles.

i. Concentrations. We used the same reactor concentrations as those employed by Hudson et al.:[5,6] $[MA]_0 = 0.3$ M, $[BrO_3^-]_0 = 0.14$ M, $[Ce^{3+}]_0 = 0.001$ M, $[H_2SO_4]_0 = 0.2$ M. However, in contrast to the Hudson experiments in which each chemical was pumped in a separate channel of the peristaltic pump, we used only three feedlines. In most experiments sulfuric acid was evenly distributed among the three feedlines, while the other components were pumped through their individual feedlines at concentrations that were 3 times more than the desired reactor concentrations.

The experiments were begun each day with freshly degassed solutions to avoid the formation of bubbles, which can produce a significant change in the residence time. The partial pressure of dissolved air, water vapor, and the continuously produced carbon dioxide together surpasses the atmospheric pressure, and that initiates bubble formation. Carbon dioxide alone, however, does not form bubbles because it is continuously removed from the CSTR by the flow.

During the course of each experiment there was a small (less than 1%) drift in the flow rate corresponding to the various transitions. This change probably was caused by oxygen gradually being dissolved in the solutions.

B. Apparatus. Reactor. A schematic drawing of the reactor is shown in Figure 1. An important feature of the construction is that the middle section of the reactor can be changed to vary the reactor volume and geometry. For most experiments the volume of the reactor was 10.7 cm^3. In one series of experiments it was 15.9 cm^3.

(7) (a) Roux, J. C.; Simoyi, R. H.; Swinney, H. L. *Physica* **1983**, *8D*, 257. (b) Roux, J. C.; Turner, J. S.; McCormick, W. D.; Swinney, H. L. In *Nonlinear Problems: Present and Future*; Bishop, A. R., Campbell, D. K., Nicolaenko, B., Eds.; North-Holland: Amsterdam, 1982; p 409. (c) Turner, J.; Roux, J. C.; McCormick, W. D.; Swinney, H. L. *Phys. Lett. A* **1981**, *85*, 9. (d) Coffman, K. C.; McCormick, W. D.; Noszticzius, Z.; Simoyi, R. H.; Swinney, H. L. *J. Chem. Phys.* **1987**, *86*, 119.

(8) Györgyi, L.; Field, R. J. *J. Chem. Phys.* **1990**, *93*, 2159.

(9) Münster, A.; Schneider, F. W. *J. Phys. Chem.* **1991**, *95*, 2130.

(10) Györgyi, L.; Field, R. J. *J. Phys. Chem.* **1989**, *93*, 2865.

(11) Györgyi, L.; Rempe, S. L.; Field, R. J. *J. Phys. Chem.* **1991**, *95*, 3159.

(12) (a) Roux, J. C.; Rossi, A.; Bachelart, S.; Vidal, C. *Phys. Lett.* **1980**, *77A*, 391. (b) Pomeau, Y.; Roux, J. C.; Rossi, A.; Bachelart, S.; Vidal, C. *J. Phys. Lett.* **1981**, *42*, L271. (c) Argoul, F.; Arneodo, A.; Richetti, P.; Roux, J. C. *J. Chem. Phys.* **1987**, *86*, 3325. (d) Ibison, P.; Scott, S. K. *J. Chem. Soc., Faraday. Trans.* **1990**, *86*, 3695.

(13) Györgyi, L.; Field, R. J. *J. Phys. Chem.* **1991**, *95*, 6594.

(14) Noszticzius, Z.; McCormick, W. D.; Swinney, H. L. *J. Phys. Chem.* **1987**, *91*, 5129.

(15) Noszticzius, Z.; McCormick, W. D.; Swinney, H. L. *J. Phys. Chem.* **1989**, *93*, 2796.

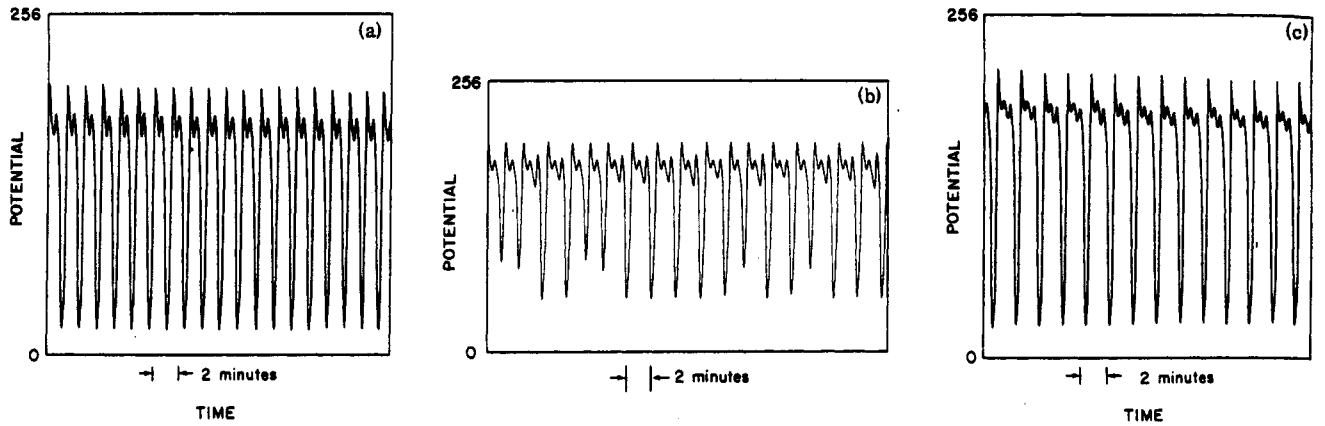

Figure 2. Chaotic state and two nearby periodic states as reported by Hudson and Mankin.[6] Recording from bromide ion electrode: (a) periodic 1^1 state, residence time of 6.35 min; (b) chaotic state between the 1^1 and 1^2 periodic windows, residence time of 6.01 min; (c) periodic 1^2 state, residence time of 5.68 min. The amplitude of the relaxation oscillations was about 41–42 mV for the periodic states according to Hudson et al.[5]

TABLE I: Residence Times for Different States Reported by Hudson et al.[5] and by Hudson and Mankin[6] and Also Found in the Present Experiments[a]

	motif											
expt	1	1^11	1^1	C	1^2	C	1^3	C	1^4	long	sin	ss
Hudson et al.[5]	8.73	6.75	6.26	5.89	5.85	5.63	5.50	5.34	5.28	4.73	4.69	4.62
Hudson and Mankin[6]			6.35	6.01	5.68							
present expts	8.72	7.08	6.49	6.23	5.89	5.70	5.53	5.45	5.42	4.84	4.74	4.64

[a] "L" denotes a combination of large (L) and small (s) oscillations. Residence times for experiments by Hudson et al. were calculated by dividing their reactor volume (25.4 mL) by the reported flow rates (in mL/min). "C" denotes chaotic behavior, and "sin" and "ss" stand for small-amplitude sinusoidal oscillations and for stable steady states, respectively. The notation "long" indicates a chaotic state where a large-amplitude relaxation oscillation is followed by a long quiescent period and then a variable number of growing small oscillations.

i. Stirrer. The stirrer was a three-bladed glass propeller driven by a synchronous motor. The usual stirring rate was 1800 rpm, but with a variable frequency power supply the stirring rate could be varied from 600 to 1800 rpm.

ii. Pumps. In most experiments three LDC/Milton Roy piston pumps were used. These were dual-piston pumps of very high precision with wetted parts composed of inert materials (glass, Teflon, and Kel-F). In some experiments a four-channel peristaltic pump (Ismatec) was used for comparison.

iii. Electrodes. A platinum (Corning 476060) bromide ion-selective electrode[16] and a double-junction Ag/AgCl reference (Sensorex) electrode were used. The solubility limit potential of the bromide selective electrode was determined as the mean of the electrode potentials measured in 10^{-5} M Ag^+ and 10^{-5} Br^- solutions mixed with 0.2 M H_2SO_4. That potential was 219 ± 1 mV for all measurements. It served as an inner reference potential to calculate bromide concentrations from electrode potentials.

iv. Temperature. The reactor was placed into a thermostated bath, and the input chemicals were brought to the same temperature by pumping through about a 1-m length of Teflon tubing placed in the bath. The temperature inside the reactor was 25.00 ± 0.05 °C, as measured by a thermistor probe that was mounted temporarily in place of the platinum electrode. It was found that, due to the exothermic reaction, the average temperature of the reactor was about 0.1 °C higher than that of the surrounding bath. Thus, the bath temperature was set to 24.9 °C. It was also found that the long relaxation portion of a typical oscillation, during which the autocatalytic reaction was switched off, was associated with a temperature drop of about 0.02 °C.

v. Electronics. Electrode potentials were amplified with high input impedance amplifiers and were recorded on a personal computer equipped with a 12-bit analog to digital converter board (MetraByte Dash-8) using the Labtech Notebook program. The sampling rate was 4 Hz, and a moving average of four samples was stored on the computer.

(16) Noszticzius, Z.; Wittmann, M.; Stirling, P. *4th Symposium on Ion-Selective Electrodes*; Pungor, E., Ed.; Elsevier: Amsterdam, 1985; p 579.

III. Results

A. Reproduction of the Hudson Experiments. Figure 2 shows time series for three of the states observed by Hudson et al., and Figure 3 shows the corresponding time series obtained in our experiments. The waveforms in Figures 2 and 3 are remarkably similar, and, moreover, the residence times at which we observe these and other states agree with those of Hudson et al.[5,6] within a few percent (see Table I). Hudson et al. give residence times for different states but not for the bifurcation points, but most complex periodic and aperiodic states exist for parameter ranges of only a few percent or less. The largest difference between their parameter values (for the state 1^11) and ours is only 5%, comparable to the combined uncertainty in their flow rate (2%) and ours (1%); our resident times are all slightly larger than those of Hudson et al.

To be certain that the remarkable correspondence of our results with those of Hudson et al. was not fortuitous, we examined the sensitivity of the observed sequence of transitions to changes in parameters that are usually held fixed. We now describe those experiments.

B. Sensitivity of the Dynamics to Some Unconventional Parameters. We studied the effect of varying the following experimental parameters: (i) the purity of the chemicals; (ii) the feeding of the chemicals (different types of pumps and premixing); (iii) the reactor size and geometry; and, most importantly, (iv) the stirring rate.

i. Impurities. While CSTR BZ systems can be very sensitive even to trace amounts of impurities, fortunately this is not the case with the present experiments. Less than 1% shift in residence times was found using uncrystallized malonic acid and bromate instead of recrystallized chemicals. The best way to observe the shift was to place the system close to the Hopf bifurcation point and to detect the appearance or the disappearance of the sinusoidal oscillations as the feed was changed from a pure to a contaminated sample or vice versa. Then the flow rate of the pump was changed to restore the original state and to measure the shift caused by the contaminant. Of course, samples that are more contaminated than ours might produce larger shifts; to avoid such uncertainties, it would certainly be desirable to recrystallize the malonic acid

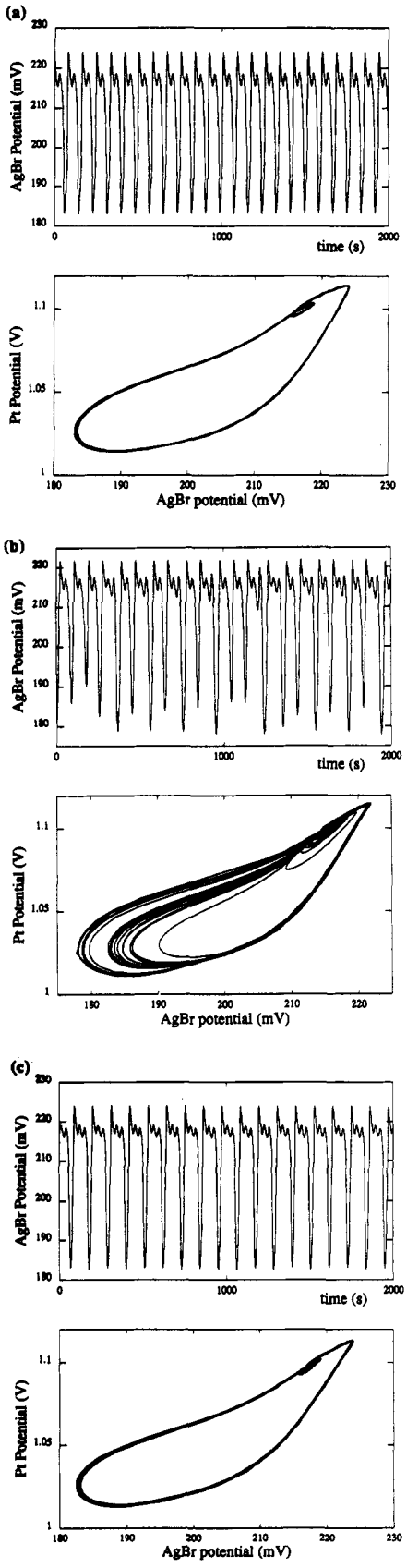

Figure 3. Time series and phase portraits obtained in the present experiments for the three states displayed in Figure 2. The phase portraits were obtained by plotting the potential of the platinum electrode as a function of the simultaneously measured bromide electrode potential: (a) periodic 1^1 state, residence time of 6.49 min; (b) chaotic state, residence time of 6.23 min; (c) 1^2 periodic state, residence time of 5.89 min. The amplitude of the periodic oscillations is 41–42 mV. The 183-mV minimum potential corresponds to a 3.6–3.8 × 10^{-6} M bromide concentration maximum.

and the bromate. What is most important, however, is that a second recrystallization of the malonic acid or the bromate produced no detectable difference compared to experiments carried out with samples recrystallized only once. This indicates that chemicals recrystallized only once are pure enough for experiments in this parameter range. As has been mentioned, cerous sulfate was not recrystallized, but high-purity cerous sulfate was used. Some cerous sulfates may contain impurities. For example, a low-purity cerous sulfate sample gave a 3% shift (decrease) in residence time compared to the high-purity Aldrich cerous sulfate used in our experiments.

ii. Feeding of Chemicals. While peristaltic pumps are convenient and inexpensive, they do periodically modulate the flow rate. There has been some speculation about the dynamic role of the periodic perturbation caused by a peristaltic pump.[17,18] Thus, we conducted experiments with peristaltic and with dual-piston pumps. With manometers inserted into the feedlines we could see that the piston pump produced a continuous flow and the peristaltic pump generated an oscillating flow. In spite of this difference, we could detect no change in the periodic or chaotic states or in the position of the bifurcation points.

The behavior was also insensitive to the premixing of sulfuric acid in different feedlines. It made no difference if all of the sulfuric acid was added to the malonic acid instead of its being distributed evenly among the three feedlines. In this respect it is interesting to point out that Hudson et al.[5,6] introduced the sulfuric acid in a separate fourth channel. In spite of this difference, their results were essentially the same.

iii. Reactor Volume and Geometry. We increased the reactor size from 10.7 to 15.9 cm^3 (see Figure 1). After this change, the various periodic and chaotic states remained the same and occurred at the same residence times within the 1% experimental uncertainty. This also shows that although the reaction is exothermic, the reactor temperature is well controlled. According to our measurements, a 0.1 °C increase in the temperature causes a 1.3% downward shift in the residence times.

iv. Stirring. According to some recent publications, stirring has an effect on the BZ reaction not only in CSTRs but in batch reactors as well.[19-21] In batch systems stirring effects are attributed to radical–radical reactions whose effect is strong when the radicals are in low concentration. In the present experiments the system is close to the oxidized steady state and the radical concentration is relatively high. Thus, stirring effects, if they occur, in this case should be attributed most probably to an incomplete mixing. In actuality, the system proved to be rather insensitive to stirring.

We studied the effect of stirring on the three different states depicted in Figure 3. No measurable change in the waveforms or transition residence times was observed for stirring rates of 1800, 1500, and 1200 rpm. A barely detectable shift, less than 1%, in the transition residence times was found for a stirring rate of 900 rpm. At 600 rpm the sequence of transitions was unchanged, but the residence times for the transitions were shifted upward by 1%. We conclude that the stirring itself and the fluctuations in stirring do not affect the dynamical behavior observed with stirring at 1800 rpm.

IV. Model Calculations and Discussion

The experiments were simulated using the four-variable model of the BZ reaction recently developed by Györgyi and Field.[13] This model reproduces the low flow rate regime very well. Table II shows the model, rate constants, and feed concentrations used in the simulations. The mixed-feed concentrations are the same as those in the experiments, and $[H^+]$ is estimated using the data

(17) Showalter, K.; Noyes, R. M.; Bar-Eli, K. *J. Chem. Phys.* **1978**, *69*, 2514.
(18) Ganapathisubramanian, N.; Noyes, R. M. *J. Chem. Phys.* **1982**, *76*, 1770.
(19) Sevcik, P.; Adamcikova, L. *Chem. Phys. Lett.* **1988**, *146*, 419.
(20) Menzinger, M.; Jankowski, P. *J. Phys. Chem.* **1990**, *94*, 4123.
(21) Noszticzius, Z.; Bodnar, Z.; Garamszegi, L.; Wittmann, M. *J. Phys. Chem.* **1991**, *95*, 6575.

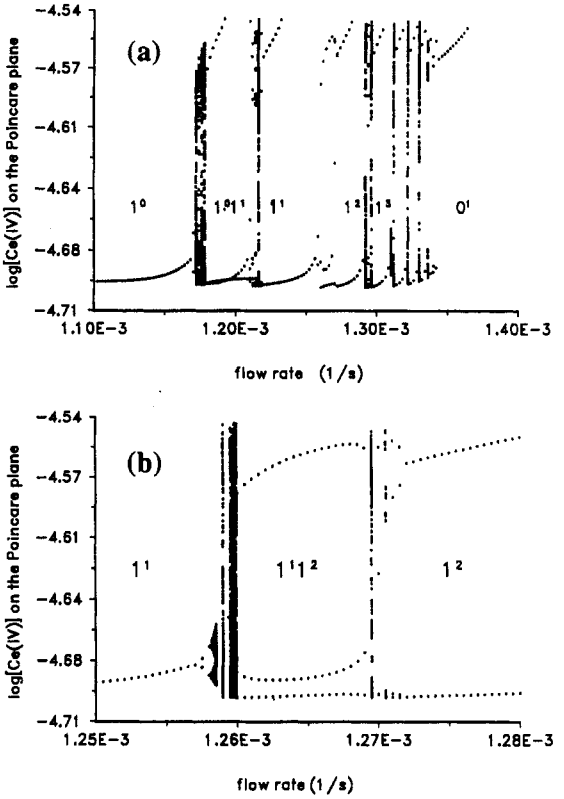

Figure 4. Bifurcation diagrams obtained for high CSTR flow rates in simulations based on the model in Table II: (a) full region of complexity at high flow rates. (b) magnification of the region between the 1^1 and 1^2 limit cycles. The log [Ce(IV)] values on the ordinate are intersections of simulated trajectories with the Poincaré plane perpendicular to the [Br^-] axis and containing the point ([Br^-] = 1.32586 × 10^{-5} M, [$HBrO_2$] = 2.71200 × 10^{-6} M, [Ce(IV)] = 2.75394 × 10^{-4} M, [BrMA] = 1.51083 × 10^{-3} M) when [Br^-] was decreasing. Results are shown when the flow rate is increased in small steps. A reverse scan revealed hysteresis between sinusoidal, 0^1, and mixed-mode oscillations, as described in the text. Periodic behavior is indicated when only a few intersections are visible at a particular k_f, while many intersections indicate chaos.

of Robertson and Dunford.[22] The set of differential equations used in the calculations was formed using the reaction rates in Table II with the addition of appropriate CSTR flow terms. The differential equations were integrated with the numerical integrator LSODE[23] with a relative error tolerance of 10^{-8}–10^{-10} and an absolute error tolerance of 10^{-16}–10^{-20}. Poincaré sections were calculated using a slight modification of the algorithm of Parker and Chua.[24] The intersections of calculated trajectories with the chosen Poincaré plane were determined to an accuracy of ±5 × 10^{-5} s.

Figure 4a shows the bifurcation sequence in the high flow rate region, simulated by the model in Table II. The presence of only a few points at a particular flow rate indicates a periodic state, while the presence of many intersections indicates chaos. This diagram is complicated because the oscillations can be composed of collections of small- and large-amplitude cycles in each period. Points at high log [Ce(IV)] are from the intersection of small-amplitude cycles with the Poincaré plane. The abrupt end of the lines of plane intersections within periodic windows (e.g., at 1.234 × 10^{-3} s^{-1}) are not bifurcations; rather, they correspond to the disappearance of intersections as the shape of oscillation changes.

Several complex periodic and chaotic regimes, indicated in Figure 4a, are between regular, 1^0, oscillations at k_f = 1.10 × 10^{-3} s^{-1} (residence time, t_r = 15.15 min) and the oxidized steady state at k_f = 1.40 × 10^{-3} s^{-1} (t_r = 11.90 min). Chaotic mixed-mode

TABLE II: Chemical Scheme of the Four-Variable Model of the BZ Reaction Used in the Simulations[a]

	rates (r_i) and rate constants (k_i)
(1) $Br^- + HBrO_2 + \{H^+\} \rightarrow 2BrMA$	$r_1 = k_1[H^+][Br^-][HBrO_2]$ k_1 = 2.0E+6 M^{-2} s^{-1}
(2) $Br^- + \{BrO_3^-\} + \{2H^+\} \rightarrow BrMA + HBrO_2$	$r_2 = k_2[BrO_3^-][H^+]^2[Br^-]$ k_2 = 2.0 M^{-3} s^{-1}
(3) $2HBrO_2 \rightarrow BrMA$	$r_3 = k_3[HBrO_2]^2$ k_3 = 3000 M^{-1} s^{-1}
(4) 0.5 $HBrO_2 + \{BrO_3^-\} + \{H^+\} \rightarrow HBrO_2 + Ce(IV)$	$r_4 = k_4[H^+]([Ce]_{tot} - [Ce(IV)])[BrO_2^\bullet]_{EQ}$ k_4 = 6.2E+4 M^{-2} s^{-1}
(5) $HBrO_2 + Ce(IV) \rightarrow 0.5\ HBrO_2$	$r_5 = k_5[HBrO_2][Ce(IV)]$ k_5 = 7000 M^{-1} s^{-1}
(6) $Ce(IV) + \{MA\} \rightarrow$	$r_6 = k_6[MA][Ce(IV)]$ k_6 = 0.3[b] M^{-1} s^{-1}
(7) $BrMA + Ce(IV) \rightarrow Br^-$	$r_7 = k_7[Ce(IV)][BrMA]$ k_7 = 30.0[b] M^{-1} s^{-1}
(8) $BrMA \rightarrow Br^-$	$r_8 = k_8[BrMA][MA^\bullet]_{QSS}$ k_8 = 2.4E+4[b] M^{-1} s^{-1}

[a] The differential equations and the origin of the rate constants for this model are given in ref 13; BrO_3^-, H^+, and MA have fixed concentrations. Chemical conditions (as in experiments): [BrO_3^-] = 0.14 M, [MA] = 0.3 M, $[Ce]_{tot}$ = 0.001 M, [H^+] = 0.26 M. The braces indicate pool chemicals. MA ≡ $CH_2(COOH)_2$. $MA^\bullet$ ≡ $^\bullet CH(COOH)_2$. BrMA ≡ $BrCH(COOH)_2$. $[MA^\bullet]_{QSS} = \{-k_8[BrMA] + ((k_8[BrMA])^2 + 2.4 \times 10^{10} k_6[MA][Ce(IV)])^{0.5}\}/(1.2 \times 10^{10})$. $[BrO_2^\bullet]_{EQ} = \{7.9 \times 10^{-7}[BrO_3^-][H^+][HBrO_2]\}^{0.5}$ [b] Adjustable rate constant.

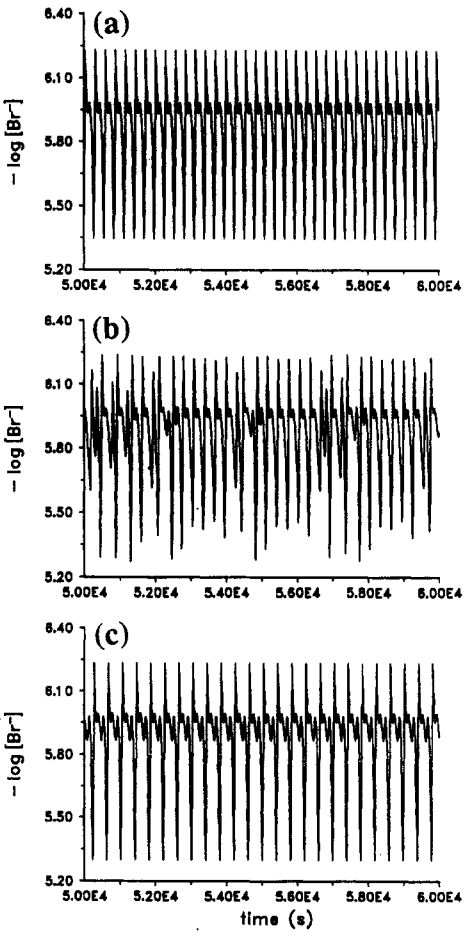

Figure 5. Typical time series from the region shown in Figure 4b: (a) 1^1 periodicity at k_f = 1.25 × 10^{-3} s^{-1}; (b) deterministic chaos at k_f = 1.259 × 10^{-3} s^{-1}; (c) 1^2 periodicity at k_f = 1.28 × 10^{-3} s^{-1}.

oscillations develop from the standard 1^0 limit cycle as the flow rate is increased to 1.172 × 10^{-3} s^{-1} (t_r = 14.22 min). One period-doubling bifurcation is observed before the onset of chaos. Several periodic and chaotic windows follow as the flow rate is increased. The most important of these are indicated in Figure

(22) Robertson, E. B.; Dunford, H. B. *J. Am. Chem. Soc.* **1964**, *86*, 5080.
(23) Technical Report UCID-3001, 1972; Lawrence Livermore Laboratory, Livermore, CA.
(24) Parker, T. S.; Chua, L. O. *Practical Numerical Algorithms for Chaotic Systems*; Springer-Verlag: New York, 1989; Chapter 2.

4a and consist of one large-amplitude and one or more small-amplitude oscillations per cycle. A magnification of the region between the 1^1 and 1^2 periodicities is shown in Figure 4b, and three corresponding time series (1^1-type limit cycle, chaos, 1^2-type limit cycle) are plotted in Figure 5. It is apparent, even with the coarse control parameter grid used for the calculations shown in Figure 4a, that chaos is found between the periodic windows. There are also several very complex periodic states that are combinations of the two neighboring 1^x-type limit cycles. Figure 4a shows the position of a 1^11^0 limit cycle, and Figure 4b shows that of a 1^11^2 periodic state. Other, more complex limit cycles, as well as oscillations derived from 1^x periodicities via period-doubling bifurcation, were also seen. Some of the chaotic attractors result from a sequence of period-doubling bifurcations from 1^x limit cycles, as, for example, is apparent in Figure 4b.

As the flow rate is increased, the number of small oscillations within a period increases, and the width of the periodic windows decreases. Some of the small peaks in the $-\log [Br^-]$ time series degenerate into shoulders; thus, the notation L^s is ambiguous in this region. The 1^8 periodicity is the last mixed-mode limit cycle seen in the simulations before an abrupt switching at $k_f = (1.344 \pm 0.001) \times 10^{-3}$ s^{-1} ($t_r = 12.40$ min) to small-amplitude, sinusoidal oscillations around the oxidized steady state, which is itself attained at a slightly higher flow rate. The only hysteresis detected in the simulations occurs when the flow rate is then decreased from the region where the oxidized steady state is dominant. The switch back to mixed-mode oscillations does not occur until $k_f = (1.332 \pm 0.001) \times 10^{-3}$ s^{-1} ($t_r = 12.51$ min). This switching is preceded by a period-doubling bifurcation. Thus, there is bistability between small-amplitude sinusoidal oscillations and mixed-mode oscillations in this region.

These simulations based on a chemically reasonable mechanism agree with the experiments in their gross features. The sequence with increasing flow rate from 1^0 oscillations to mixed-mode limit cycles, more complex periodicities with chaos between them, and small-amplitude sinusoidal oscillations before the oxidized steady state is finally reached is the same as is observed experimentally. Most importantly, the chaos observed in experiments at high flow rates is reproduced here.

The mechanistic source of complex behavior has been identified[13] at both high and low flow rates as the interaction between the usual BZ oscillations and the flow-driven cycling of bromomalonic acid. Recent studies[11,15] have shown that bromomalonic acid is a slow variable responsible for the complex behavior. Oscillations are possible only when its concentration is within a certain range.

The simulations are somewhat more detailed than the experiments. For example, only a few period-doubled states were observed experimentally, and it was not possible to determine whether the bistability between mixed-mode and sinusoidal oscillations seen in the simulations exists in the real system. In general, complex oscillations and chaos were observed experimentally at higher flow rates and over a wider flow rate range than in the simulations.

V. Conclusions

This work presents an independent experimental confirmation of the existence of deterministic chaos at high CSTR flow rates. Our results agree with those of Hudson and Mankin,[6] both in the sequence of phenomena seen as the flow rate is varied and in the absolute flow rate values where the phenomena occur. In contrast to the situation at low flow rates, certain features of the high flow rate periodic–chaotic sequence observed are found to be rather insensitive to impurities in malonic acid, to the type of pump used, to small fluctuations in reactor temperature, to reactor configuration and volume, and to the stirring rate. Simulations based on a recent model of the BZ reaction reproduce the principal characteristics of the experiments, including the appearance of chaos.

Acknowledgment. This work was partially supported by National Science Foundation Grant CHE-88-22886, by Department of Energy Office of Basic Energy Sciences Grant DE-FG05-88ER13821, and by Robert A. Welch Foundation Grant F-805. Computing facilities were supplied by the University of Montana Computing and Information Services.

Registry No. BrO_3^-, 15541-45-4; Ce, 7440-45-1; malonic acid, 141-82-2.

An EPR Study of the Reaction of ^{69}Ga Atoms with Ethylene in Hydrocarbon Matrices[1]

J. A. Howard,*

Steacie Institute for Molecular Sciences, National Research Council of Canada, Ottawa, Canada K1A 0R9

H. A. Joly,*

Department of Chemistry, Laurentian University, Sudbury, Ontario, Canada P3E 2C6

and B. Mile

School of Chemistry and Applied Chemistry, University of Wales, College of Cardiff, P.O. Box 912, Cardiff, U.K. CF1 3TB *(Received: May 13, 1991; In Final Form: September 3, 1991)*

The reaction of ^{69}Ga atoms with ethylene in adamantane on a rotating cryostat at 77 K has been studied by EPR spectroscopy. The major paramagnetic product is the Ga atom–ethylene π complex $^{69}Ga[C_2H_4]$ that has the magnetic parameters $|a_{xx}(69)| = 242$ MHz, $|a_{zz}(69)| = 82$ MHz, $|a_{yy}(69)| = 100$ MHz, $g_{xx} = 2.0031$, $g_{zz} = 1.9807$, and $g_{yy} = 2.0107$ and has an unpaired spin population of ~0.56 in the Ga $4p_x$ orbital. These parameters are almost identical to those of $^{69}Ga[C_2H_4]$ in argon at 4 K and confirm that this complex has a $^2B_1$ electronic ground state in the point group C_{2v}. There is also a quartet of almost isotropic transitions in the spectrum with the parameters $|a_{\parallel}(69)| = 1669$ MHz, $|a_{\perp}(69)| = 1698$ MHz, $g_{\parallel} = 1.9955$, and $g_{\perp} = 1.9839$ that have been tentatively assigned to the cyclic σ-bonded complex gallacyclopentane, $\overline{GaCH_2CH_2CH_2CH_2}$.

Introduction

Ground-state Al atoms react with ethylene in adamantane on a rotating cryostat at 77 K to give two major paramagnetic products, the monoethylene monoaluminum π complex, $Al[C_2H_4]$,[2] and aluminacyclopentane, $\overline{AlCH_2CH_2CH_2CH_2}$.[3] The same re-

(1) Issued as NRCC No. 32940.

(2) Howard, J. A.; Mile, B.; Tse, J. S.; Morris, H. *J. Chem. Soc., Faraday Trans. 1* **1987**, *83*, 3701.

0022-3654/92/2096-1233$03.00/0 Published 1992 by the American Chemical Society